

Ivan I. Gorial 

Department of Control and
Systems Engineering,
Mechatronics Engineering
Branch, Technology
University, Baghdad, Iraq
ivanisho@gmail.com

Received on: 12/09/2017

Accepted on: 25/01/2018

Sliding Mode Controller Design for Flexible Joint Robot

Abstract- This paper suggests a flexible joint robot operated by brushed Direct Current (DC) motor model. Due to complex high-order, nonlinear dynamical system which operating under parameter's uncertainty, sliding mode control (SMC) used to solve this problem of control the flexible joint robot. The SMC method is identified as one of the effective method to design robust control for the flexible joint robot, which based on t using a Low Pass Filter (LPF) with suitable time constant. The mathematical model is presented clearly and the simulations together with their analysis are done using MATLAB software. Simulation results display the efficacy of the designed robust control in stabilizing the system states and forcing the link side angle to converge to the desired value with appropriate control effort.

Keywords- SMC, Flexible joint robot, DC-motor, LPF.

How to cite this article: I.I. Gorial, "Sliding Mode Controller Design for Flexible Joint Robot," *Engineering and Technology Journal*, Vol. 36, Part A, No. 7, pp. 733-141, 2018.

1. Introduction

By depending on their make, robot manipulators classified as flexible and rigid. Rigid manipulators have raised tensile strength with more precision because of the material utilized. However, the technology progression in material has permitted low weight and cost, which demands adaptive or robust control laws to deal with trajectories [1]. Flexible manipulators display numerous advantages over their traditional rigid ones: their motors are smaller, light weight, frugal production, and consume less energy. As a result of these imperative highlights, applications of flexible manipulators are exceedingly created, and accomplished a critical part in numerous science domains, for example, operation of surgical [2,3], application in nuclear [4], and structures of aerospace [5,6]. Joint flexibility is an important factor to consider in the controller design for robot manipulators if high performance is expected. In the recent years, significant research efforts have been made to solve the flexible-joint robot control problem. When there is a difference between that of the driven link and the angular position of the driving actuator joint flexibility occurs. It is known that the joint flexibility can cause oscillations in robot manipulators. Therefore, it is considered as a problem [7]. Some approaches of control demand numerous feedbacks or even a precise system model [8]. The vast majority of the familiar schemes about robot manipulators control strategies are depended on one/both of these simplified assumptions: Firstly, assumption is neglecting dynamics of motor. Secondly,

assumption is neglecting the flexibility of joint [9]. Thus, like this system, mathematical and dynamic modeling analysis is significant and examined by authors as in [10] flexible manipulators dynamical behavior was analyzed depended on recursive lagrangian method. Moreover, in [11] an approach of Newton-Euler was suggested to robot flexible dynamical model. Meghdari and Fahimi [12] utilized an analytically method of elastic manipulators to decouple the equations of dynamic. Besides, Korayem et al. [13,14] supposed the flexible manipulator systems dynamical modeling. Aziz and Iqbal [15] presented modeling and control of a robotic flexible arm with single DOF where Euler-Lagrange based method was derived for this model. Jafari et al. [16] presented flexible manipulator depended on method of finite element. Chang and Yen [17] addressed the motion tracking control for a category of flexible-joint robotic. Izadbakhsh [8] addressed Lyapunov design for flexible joint robots controller based electrically driven as control - input to voltage. Furthermore, because of uncertainty and existence of the nonlinear components in its dynamical model, SMC theory was used by many authors as for the throttle valve angle control system, by AL-Samarraie [18]. AL-Samarraie and AL-Wardie [19] proposed a new SMC design for the electromechanical system without neglecting the inductance in the electrical part or approximating the non-smooth perturbation but by transforming the electrical part to a low-pass filter by a primary control design. The uncertainty in system model parameters is the problem for the application of many control theories. The sliding

<https://doi.org/10.30684/etj.36.7A.5>

2412-0758/University of Technology-Iraq, Baghdad, Iraq

This is an open access article under the CC BY 4.0 license <http://creativecommons.org/licenses/by/4.0>

mode control method can be solved this problem [20]. Now, a great motion control amount is accomplished utilizing electric motors, for this reason, it will be our essential consideration. In the design, motion control systems can be quite complicated because various factors have to be taken into account. The following issues should ordinarily be considered: disturbances, attenuation and uncertainties, i.e. concise these factors as the uncertainty in system model parameters, non-smoothness in its model, nonlinearity, and non-satisfying matching condition [19]. In [21] to build a dynamic structure, utilized the output and its derivatives estimation and in [22], a SMC applied in crane system to overcome uncertainties. The aim of this study was to suggest a new method to design controller for flexible joint robot. Firstly, the controller designed to transform the electrical system to LPF with a suitable small time constant. Secondly, a control law derived for the mechanical system utilizing theory of SMC, after linearizing the mechanical system model, which it is capable to force the mechanical state to the desired reference in spite of the presence of uncertainty system model.

2. Mathematical Model

The dynamic equation of the flexible joint single link manipulator driven electrically as clarified in Figure 1 can be modelled mathematically as the following equations:

For the link, the mathematical model based on Newton's law is [9, 23];

$$\left. \begin{aligned} I\ddot{\theta} &= -mgl \sin(\theta) - K(\theta - \theta_m) \\ \text{or} \\ \ddot{\theta} &= \frac{1}{I}(-mgl \sin(\theta) - K(\theta - \theta_m)) \end{aligned} \right\} \quad (1)$$

Generally, the torque resulted from a DC motor is proportional to I_a , and magnetic field strength. Let's say constant magnetic field, T_m proportional to only I_a by K_m as interpreted in the following equation:

$$T_m = K_m I_a$$

where the controller for armature-DC motor system is the input voltage e_a , e_b is proportional to the angular velocity of the shaft by a constant factor K_b .

$$e_b = K_b \omega = K_b \dot{\theta}_m(t)$$

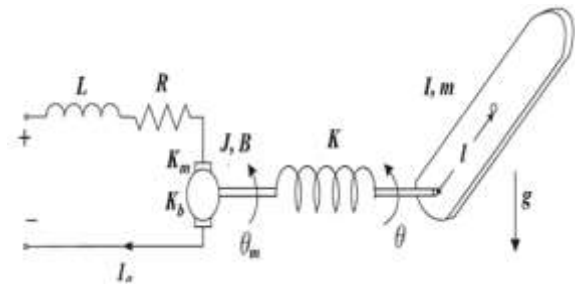


Figure 1: Flexible joint single link manipulator driven by brushed DC motor [9]

For motor, the mathematical model depending on Newton's 2nd law and Kirchoff's voltage law for Figure (1), the equations derived is as follows:

$$\left. \begin{aligned} J\ddot{\theta}_m &= T_m(t) - B\dot{\theta}_m + T(t) = K_m I_a - \\ & \quad B\dot{\theta}_m(t) + K(\theta - \theta_m) \\ \text{or} \\ \ddot{\theta}_m &= \frac{1}{J}(K_m I_a - B\dot{\theta}_m(t) + K(\theta - \theta_m)) \end{aligned} \right\} \quad (2)$$

And for armature circuit:

$$e_a(t) - R_a I_a - L_a \frac{dI_a}{dt} - e_b(t) = 0$$

which leads

$$I_a = \frac{1}{L_a}(-K_b \dot{\theta}_m(t) + e_a(t) - R_a I_a) \quad (3)$$

According to the above equations, the state vector includes angular position, angular velocity for both link and motor and the current of motor is:

$$\begin{aligned} x_1 &= \theta, \dot{x}_1 = \dot{\theta} = x_2; \dot{x}_2 = \ddot{\theta} \\ x_3 &= \theta_m \\ \dot{x}_3 &= x_4 = \dot{\theta}_m; \dot{x}_4 = \ddot{\theta}_m \\ I_a &= x_5 \end{aligned}$$

Therefore, the mathematical model in state space form becomes;

$$\begin{aligned} \dot{x}_1 &= x_2 \quad (4) \\ \dot{x}_2 &= \frac{1}{I}(-mgl \sin(x_1) - K(x_1 - x_3)) \end{aligned} \quad (5)$$

$$\dot{x}_3 = x_4$$

$$(6)$$

$$\dot{x}_4 = \frac{1}{J}(K_m x_5 - Bx_4 + K(x_1 - x_3)) \quad (7)$$

$$\dot{x}_5 = \frac{1}{L_a}(-K_b x_4 + e_a(t) - R_a x_5)$$

$$(8)$$

Where the mechanical system interpreted by equations (4) - (7), while the electrical system interpreted by the equation (8). Table (1) shows DC motor parameters.

Table 1: System parameters values utilized in numerical solutions [9, 23]

Parameters	Definition	Values	Unit
mgl	m : mass of link; l : length of the link	5	(Nm)
I	Link inertia coefficient	1	(Kg.m ²)
$I_a(t)$	Armature current		(A)
L_a	Armature inductance	0.01	(H)
R_a	Armature resistance	1.6	(Ω)
$T_L(t)$	Load torque		(N.m)
$T_m(t)$	Motor torque		(N.m)
$\theta_m(t)$	Rotor displacement		radian
K_m	Torque constant	0.2	(Nm/A)
K	Joint stiffness coefficient	100	(Nm/rad)
$e_a(t)$	Applied voltage		(V)
$e_b(t)$	Back emf		(V)
K_b	Back emf constant	0.26	(Nm/A)
$J_m(t)$	Rotor inertia	0.3	(Kg.m ²)
$B_m(t)$	Viscous-friction coefficient	0.001	(Nm.s/rad)

3. Sliding Mode Control Design for Suggested System

SMC is a nonlinear control strategy that changes the dynamics of a nonlinear system. For its ability to refuse the system model uncertainties and to the external disturbances that satisfying the matching condition, it is known robust mechanism [24]. The objective of the designed controller is to drive the system states to the origin; this actually can be done by introducing a new output function and design the controller to constrain the states movement within the neighborhood of this switching surface. The essential idea of designing SMC algorithms comprises in two steps: Firstly, choosing a manifold in state space. Secondly, designing a discontinuous control and stay there for all future time. The chattering attitude which frequently appears in SMC system for many causes like the nonideality of the switching [25]. Typical example for second order system illustrated in Figure 2 [26].

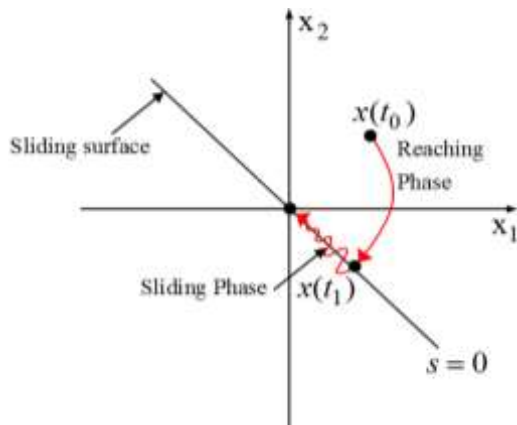


Figure 2: Typical example for second order system [26]

SMC operated by switching the trajectory of the system from one structure to other and in between sliding on a particular line, surface or plane in state space. The system trajectory motion along a selected path in state space known the sliding mode and the controller designed with the aim to investigate the sliding motion known SMC. It is chosen because it provides robustness and quick dynamics [27,28]. The control design approach presented in this work is beginning by transforming the flexible joint single link manipulator to fourth order canonical form with which the SMC can be designed. To do that the electrical subsystem equation (8) is transformed to a LPF with suitable time constant via the following primary control design;

Let,

$$f_5(x) + g_5(x)u = \frac{1}{T}(-x_5 + u_1)$$

Where, from equation (8): $f_5 = \frac{1}{L_a}(-K_b x_4 - R_a x_5)$, $g_5 = \frac{1}{L_a}$, $u = e(t)$ and u_1 is a control term to be designed later.

Accordingly, equation (8) becomes;

$$\dot{x}_5 = \frac{1}{T}(-x_5 + u_1) \tag{9}$$

And the control u is determined as;

$$u = \frac{1}{g_5(x)} \left\{ -f_5(x) + \frac{1}{T}(-x_5 + u_1) \right\}, \quad g_5(x) \neq 0 \quad \forall x \tag{10}$$

where T : time constant (selected) for the LPF resulted by the controller u , where it is assumed that f_5, g_5 (primary control design) are known without uncertainty. To this end let us replace x_5 in equation (7) by u_1 as a step to be clarified later within the SMC context. Accordingly, the fourth order system dynamics becomes:

$$\left. \begin{aligned} \dot{x}_1 &= x_2 \\ \dot{x}_2 &= \frac{1}{I}(-mgl \sin(x_1) - K(x_1 - x_3)) \\ \dot{x}_3 &= x_4 \\ \dot{x}_4 &= \frac{1}{J}(-Bx_4 + K(x_1 - x_3)) + \frac{K_m}{J} u_1 \end{aligned} \right\} \dots (11)$$

Equation (11) is linearized [29] via the following error function:

$$\left. \begin{aligned} e_1 &= x - x_d \\ \text{or} \\ e_1 &= x_1 - x_{1d} \\ e_2 &= \dot{x}_1 - \dot{x}_d = \dot{e}_1 \\ e_3 &= \ddot{x}_1 - \ddot{x}_d = \dot{e}_2 \\ e_4 &= \dddot{x}_1 - \dddot{x}_d = \dot{e}_3 \end{aligned} \right\} \tag{12}$$

where, x_d is the designed value for x and their derivative ($\dot{x}_d, \ddot{x}_d, \dddot{x}_d$) Since the relative degree is four, equation (11) is transformed to a canonical form in terms of the error function

$$\dot{e}_4 = x^{(4)}_1 - x^{(4)}_{1d} = f_4(x) + g(x)u_1 \tag{13}$$

where

$$f_4(x) = \frac{1}{I} \left(\frac{-mgl}{I} \cos(x_1) - \frac{K}{J} \right) (-mgl \sin(x_1) - K(x_1 - x_3)) + \left. \begin{aligned} & \left(\frac{mgl}{I} \sin(x_1) \times x_2^2 \right) + \\ & \frac{K}{IJ} (-Bx_4 + K(x_1 - x_3)) \end{aligned} \right\} \tilde{F}(x) = \left(\frac{-mgl}{I} \cos(x_1) - \frac{K}{J} \right) \left(\frac{-mgl \sin(x_1)}{I} - \frac{K(x_1 - x_3)}{I} \right) + \left. \begin{aligned} & \left(\frac{mgl}{I} x_2^2 \sin(x_1) \right) + \\ & \frac{K}{I} \left(-\frac{B}{J} x_4 + \frac{K}{J} (x_1 - x_3) \right) + \lambda_3 \left(\frac{-mgl}{I} x_2 \cos(x_1) - \frac{K}{I} x_2 + \frac{K}{I} x_4 \right) + \\ & \lambda_2 \left(\frac{-mgl \sin(x_1)}{I} - \frac{K(x_1 - x_3)}{I} \right) + \lambda_1 x_2 \end{aligned} \right\} \tilde{G}(x) = \frac{KK_m}{IJ}$$

Now let the sliding variable s (named also as switching function) be defined as:

$$s = e_4 + \lambda_3 e_3 + \lambda_2 e_2 + \lambda_1 e_1 \tag{14 b}$$

When switching manifold (the sliding variable($s = 0$)) reaches zero value, the error function asymptotically will decay to origin since λ_1, λ_2 and $\lambda_3 > 0$. Where, λ_1, λ_2 and λ_3 are positive design parameters.

$$0 = \ddot{e} + \lambda_3 \dot{e} + \lambda_2 e + \lambda_1 e \tag{15}$$

$$0 = m^3 + \lambda_3 m^2 + \lambda_2 m + \lambda_1 \tag{16}$$

or

$$0 = (m + a_1)(m + a_2)(m + a_3)$$

So, $m = -a_1, m = -a_2$ and $m = -a_3$

$$0 = m^3 + (a_1 + a_2 + a_3)m^2 + (a_1 a_2 + a_1 a_3 + a_2 a_3)m + (a_1 a_2 a_3) \tag{17}$$

By comparing equation (16) with equation (17) get:

$$\lambda_1 = (a_1 a_2 a_3), \lambda_2 = (a_1 a_2 + a_1 a_3 + a_2 a_3), \lambda_3 = (a_1 + a_2 + a_3)$$

Where, a_1, a_2 and a_3 are positive design parameters which are selected such that the error dynamics takes the desired characteristics. To determine the discontinuous control u_1 we need to compute \dot{s} and after that apply the sliding mode condition as follows;

$$\begin{aligned} \dot{s} &= \dot{e}_4 + \lambda_3 \dot{e}_3 + \lambda_2 \dot{e}_2 + \lambda_1 \dot{e}_1 \\ &= (\dot{x}_4 - \dot{x}_{4d}) + \lambda_3 (\dot{x}_3 - \dot{x}_{3d}) + \lambda_2 (\dot{x}_2 - \dot{x}_{2d}) + \lambda_1 (\dot{x}_1 - \dot{x}_{1d}) \\ &= \left(\frac{-mgl}{I} \cos(x_1) - \frac{K}{I} \right) \left(\frac{-mgl \sin(x_1)}{I} - \frac{K(x_1 - x_3)}{I} \right) + \left(\frac{mgl}{I} x_2^2 \sin(x_1) \right) + \\ & \quad \frac{K}{I} \left(\frac{K_m}{J} u_1 - \frac{B}{J} x_4 + \frac{K}{J} (x_1 - x_3) \right) + \\ & \quad \lambda_3 \left(\frac{-mgl}{I} x_2 \cos(x_1) - \frac{K}{I} x_2 + \frac{K}{I} x_4 \right) + \\ & \quad \lambda_2 \left(\frac{-mgl \sin(x_1)}{I} - \frac{K(x_1 - x_3)}{I} \right) + \lambda_1 x_2 \end{aligned} \tag{18}$$

$$\dot{s} = \left(\frac{-mgl}{I} \cos(x_1) - \frac{K}{I} \right) \left(\frac{-mgl \sin(x_1)}{I} - \frac{K(x_1 - x_3)}{I} \right) + \left(\frac{mgl}{I} x_2^2 \sin(x_1) \right) +$$

$$\begin{aligned} & \frac{K}{I} \left(-\frac{B}{J} x_4 + \frac{K}{J} (x_1 - x_3) \right) + \lambda_3 \left(\frac{-mgl}{I} x_2 \cos(x_1) - \frac{K}{I} x_2 + \frac{K}{I} x_4 \right) + \\ & \lambda_2 \left(\frac{-mgl \sin(x_1)}{I} - \frac{K(x_1 - x_3)}{I} \right) + \lambda_1 x_2 + \frac{KK_m}{IJ} u_1 \\ & = \tilde{F}(x) + \tilde{G}(x) u_1, \quad G > 0 \end{aligned} \tag{19 a}$$

Where,

In the certain and uncertain terms \dot{s} is rewritten as;

$$\dot{s} = G \left(\frac{F}{G} + u_1 \right) = G \left(\left(\frac{F}{G} \right)_o + \Delta \left(\frac{F}{G} \right) + u_1 \right) \tag{20 a}$$

In the next step the control law u_1 is derived that will enforce the state to reach the sliding manifold in finite time. To design u_1 , the candidate function of Lyapunov V is chosen as:

$$V = |s| \tag{20 b}$$

and its time derivative \dot{V} is:

$$\dot{V} = \text{sgn}(s) \times \dot{s}, s \neq 0 \tag{20 c}$$

This is known as the generalized derivative since the candidate Lyapunov function is non-smooth [30].

or,

$$\dot{V} = \text{sgn}(s) \times \left[\left(\frac{F}{G} \right)_o + \Delta \left(\frac{F}{G} \right) + u_1 \right] \tag{21}$$

In this paper, u_1 is selected as in the conventional sliding mode such that \dot{V} is negative definite;

$$u_1 = - \left(\frac{F}{G} \right)_o - \alpha \text{sgn}(s) \tag{22 a}$$

Then \dot{V} becomes:

$$\begin{aligned} \dot{V} &= \text{sgn}(s) \times \left[\Delta \left(\frac{F}{G} \right) - \alpha \text{sgn}(s) \right] \\ &= -\alpha + \Delta \left(\frac{F}{G} \right) \times \text{sgn}(s) \end{aligned} \tag{22 b}$$

or

$$\dot{V} \leq -\alpha + \left| \Delta \left(\frac{F}{G} \right) \right| \tag{23}$$

The gain α (must be large enough) that will make the inequality (23) less than zero (attractiveness of the sliding manifold and sliding motion). It is selected as follows:

$$\left| \Delta \left(\frac{F}{G} \right) \right| < \left| \beta \left(\frac{F}{G} \right)_o \right| \tag{24}$$

$$0 < \beta < 1$$

Substituting equation (24) in the inequality (23) and solving for α , obtain:

$$\dot{V} \leq -\alpha + \left| \beta \left(\frac{F}{G} \right)_o \right|$$

$$\alpha = \alpha_o + \beta \left(\frac{F}{G} \right)_o \tag{25}$$

Where, α_o is a positive constant.

$$\dot{V} \leq -\alpha_o$$

$$u_1 = - \left(\frac{F}{G} \right)_o - \alpha \text{sgn}(s)$$

or

$$u_1 = - \left(\frac{F}{G} \right)_o - \left(\alpha_o + \beta \left| \left(\frac{F}{G} \right)_o \right| \right) \text{sgn}(s)$$

(26)

Finally, from equation (10) and equation (26), the control law u is given by:

$$u = L_a \left(\left(-\frac{1}{T} + \frac{R_a}{L_a} \right) x_5 + \frac{k_b}{L_a} x_4 + \frac{1}{T} u_1 \right) \quad (27)$$

4. Simulation Results

The flexibility of joint can cause oscillations in manipulators so that, it is considered as a problem. A robust nonlinear controller SMC is proposed for stabilization and prevent the oscillation while the flexible joint manipulator reaches the desired angle. For system closed loop, the stability analysis is performed. The suggested controller requires information of feedback for each velocity and position on link, motor in addition to armature current. For a flexible joint single link robot as shown in Figure 1 with nominal system parameter given in Table 1, simulation results indicate a good performance of designed controller. In order to show the effectiveness of the designed controller, four simulation cases are performed for the flexible joint manipulator with single link. The simulation results in these four cases represent the system states variations, the sliding variable s and the control voltage u . All of them plotted versus time. These states are illustrated above as (x_1) , (x_2) , (x_3) , (x_4) and (x_5) respectively which are stabilized and converge to desired value. For nominal controller, λ_1 , λ_2 and λ_3 are determined based on pole placement method. The poles are selected such that the angular position on the link side reaches the desired angle without overshoot as one of the main requirements. To achieve this end, the characteristic roots for nominal system equation (16) are 2, 4 and 6 for a_1 , a_2 and a_3 respectively, then $\lambda_1 = 48$, $\lambda_2 = 44$ and $\lambda_3 = 12$. In the first case: system states initial conditions are chosen as [30; 0; 30; 0; 0] in degree and the desired angular position on the link side equal to 0 deg. In addition to the parameters values as mentioned in Table 1. Figures 3 - 5 clarify the ability of the SMC in forcing the angular position on the link side to reach the desired angle within an interval of time not exceeds 3 sec.

Figure 3: Angular position on the link side versus time

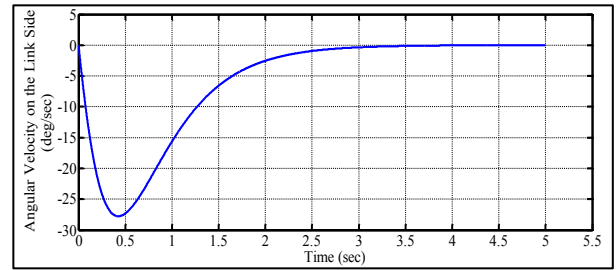


Figure 4: Angular velocity on the link side versus time

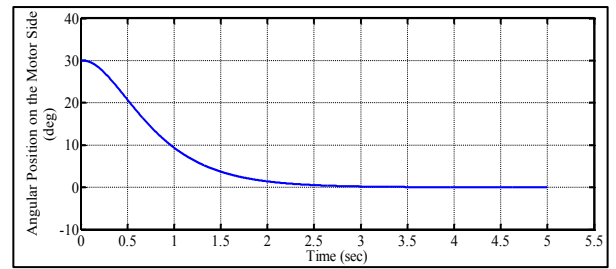


Figure 5: Angular position on the motor side versus time

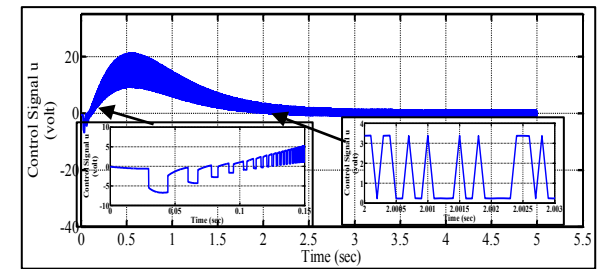


Figure 6: Sliding variable S versus time

The sliding variable oscillates around $s = 0$ is shown in Figure 6. It can also note that the sliding variable requires less than 0.1 sec to reach and stay very close to zero value.

The control signal (in voltage) is shown in Figure 7 and its value is less than 22 volts. Figure 7 reveals the high switching process of the controller due to the discontinuity nature of SMC law Eq. (29).

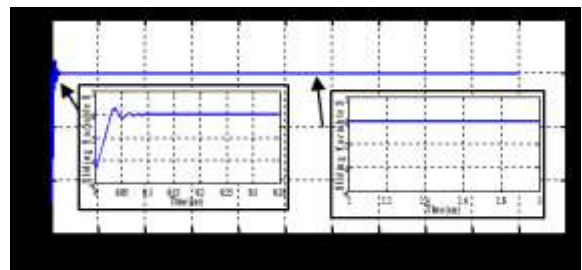
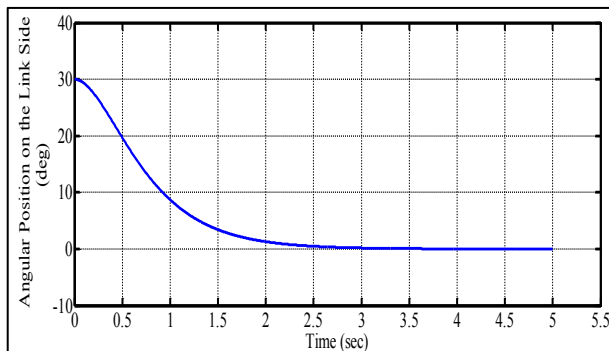


Figure 7: Control signal u versus time

When it is required to eliminate the chattering, the signum function which appears in the sliding

mode control law is replaced by an approximate function. The arc tan function is used instead of the signum function as follows:

$$\text{sign}(s) \approx \frac{2}{\pi} \tan^{-1}(rr \times s) \quad (28)$$

Where, $rr > 1$ is a design parameter adjusted in such a way that the response resembles the sliding motion but in continuous manner. So, Eq. (27) becomes:

$$u_1 = -\left(\frac{F}{G}\right)_o - \left(\alpha_o + \beta \left|\left(\frac{F}{G}\right)_o\right|\right) \times \frac{2}{\pi} \tan^{-1}(rr \times s) \quad (29)$$

The suggested system is simulated with approximate signum function according to Eq. (28) as clarified in Figures 8-11. The angular position on the link side response is very close to system response without approximation. The chattering in Figure 7 is significantly reduced compared with that in Figure 11.

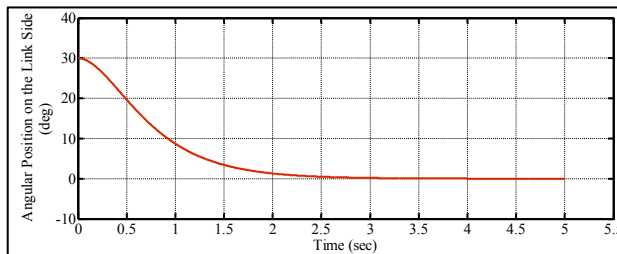


Figure 8: Angular position on the link side versus time

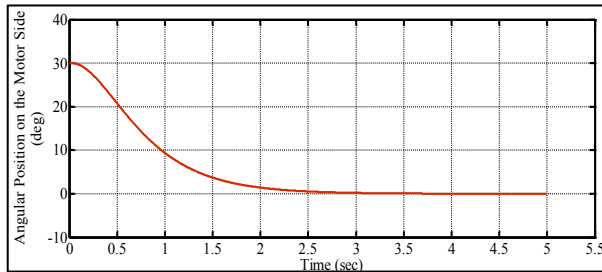


Figure 9: Angular position on the motor side versus time

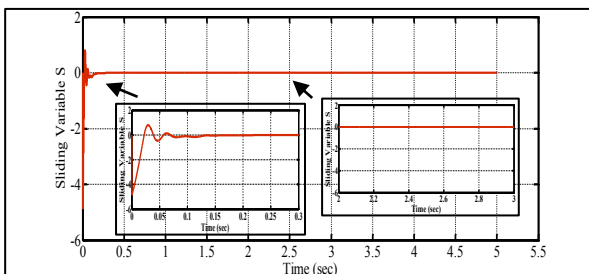


Figure 10: Sliding variable S versus time

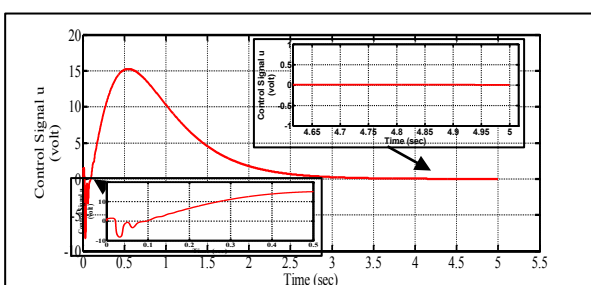


Figure 11: Control signal u versus time
In case two: system states initial conditions are chosen as [60; 0; 60; 0; 0] in degree and desired angular position on the link side equal to 60 deg. As shown in Figures 12-15, all of the states are stabilized and the link side angle converges to the desired value.

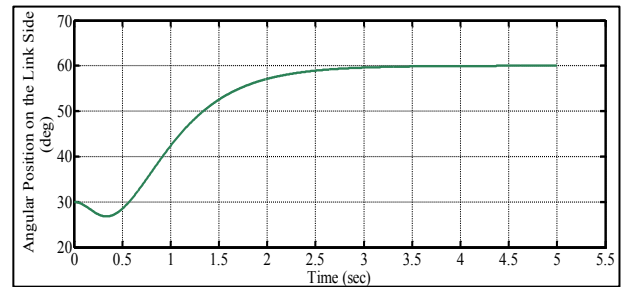


Figure 12: Angular position on the link side versus time

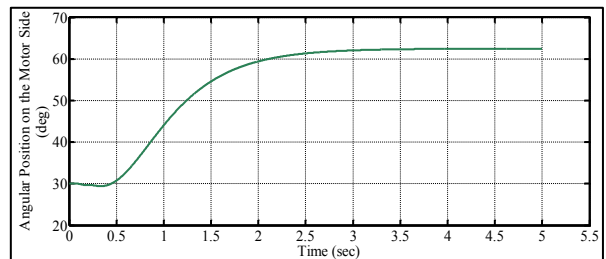


Figure 13: Angular position on the motor side versus time

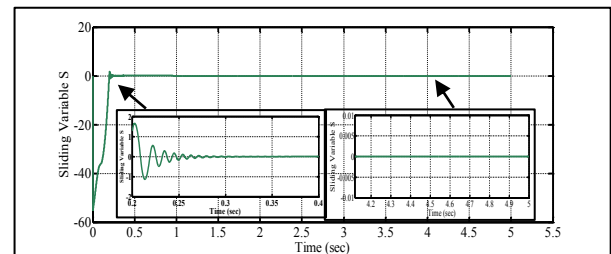


Figure 14: Sliding variable S versus time

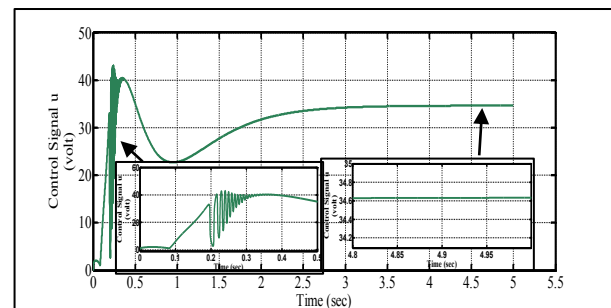


Figure 15: Control signal u versus time

In addition to case one and case two that illustrated above which are performed for nominal system parameters, in case three and case four: change in system parameters, i.e.:

$$K = 122 \text{ Nm/rad}, \quad mgl = 6 \text{ Nm}, \quad I = 1.44 \text{ Kg. m}^2$$

and $B_m = 0 \text{ Nm.s/rad}$. Also, the desired angular position on the link side is equal to 0 deg. in case three and 60deg. in case four with same system states initial conditions in case one and two which are chosen as $[30; 0; 30; 0; 0]$. Figures 16 - 19 show case three and case four respectively, all of the states are stabilized and the link side angle converges to the desired value.

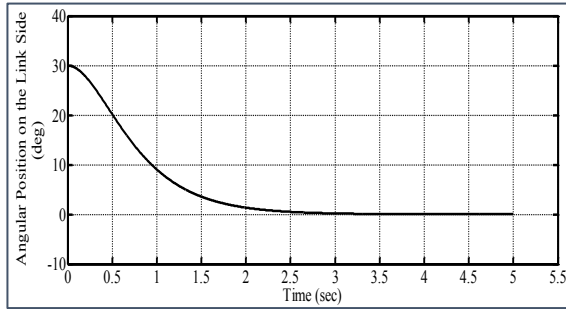


Figure 16: Angular position on the link side versus time

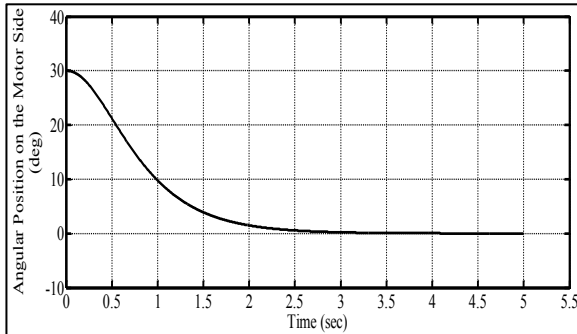


Figure 17: Angular position on the motor side versus time

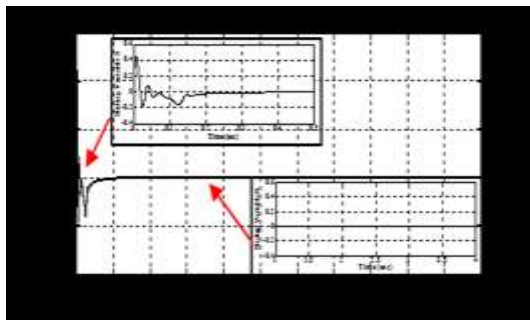


Figure 18: Sliding variable S versus time

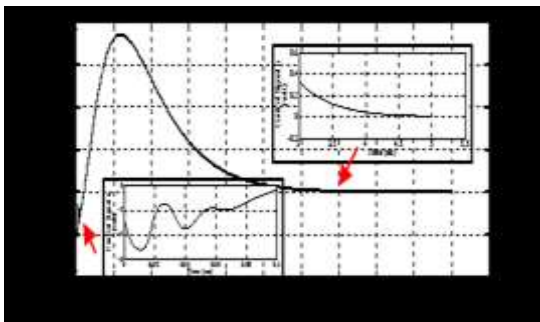


Figure 19: Control signal u versus time

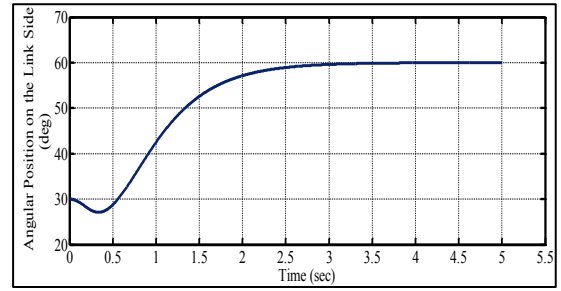


Figure 20: Angular position on the link side versus time

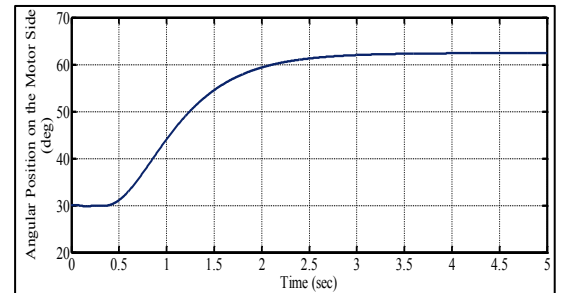


Figure 21: Angular position on the motor side versus time

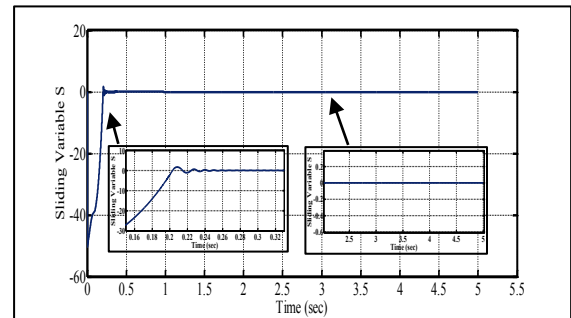


Figure 22: Sliding variable S versus time

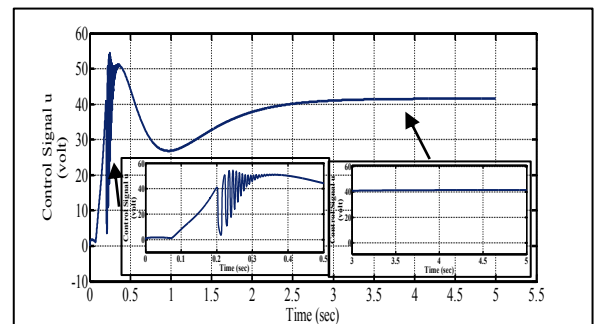


Figure 23: Control signal u versus time

Due to the flexibility of joint, the armature angle equal to 63 deg. and the link angular position equal to 60 deg. while the desired angle equal to 60 deg. as illustrated in Figure 24.

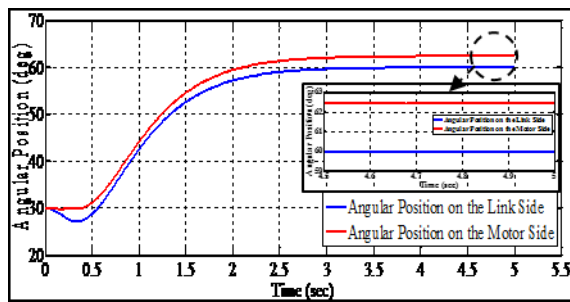


Figure 24: Angular position on the link side and angular position on the motor side versus time

5. Conclusion

Simulation results indicate the effectiveness and robustness of the suggested controller with the nonlinearity existence and uncertainty in system parameters. The uncertainty in system parameters values validate the efficacy of the suggested controller. Chattering problem is solved by replacing the signum function with arc tan function as approximation. In spite of this approximation, the time required to reach the target is still nearly equal (with suitable value for rr) as proved in simulations of these four cases. The simulation results show that the chattering is eliminated. Finally, no oscillatory motion of manipulator end-effector was observed in reaching the required angle for the link side. This suggested controller can be utilized for more comprehensive category of manipulator.

References

- [1] S. Ajwad, M. Ullah, R. Islam and J. Iqbal, "Modeling robotic arms—A review and derivation of screw theory based kinematics," International Conference on Engineering & Emerging Technologies, pp. 66-69, 2014.
- [2] H. Liao, H. Suzuk, K. Matsumiya, K. Masamune, T. Dohi and T. Chiba, "Fetus-supporting Flexible Manipulator with Balloon-type Stabilizer for Endoscopic Intrauterine Surgery," Int J of Medical Robotics and Computer Assisted Surgery, 214–223, 2008.
- [3] R. Kumar, P. Berkelman, P. Gupta, A. Barnes, P.S. Jensen, L.L. Whitcomb and R. Taylor, "Preliminary Experiments in Cooperative Human/robot Force Control for Robot Assisted Micro-Surgical Manipulation," Proc of IEEE IntConf on Robotics and Automation, 123-132, 2000.
- [4] Y. Perrot, J.J. Cordier, J.P. Friconneau et al., "Development of a long reach articulated manipulator for ITER in vessel inspection under vacuum and temperature," Fusion Eng. Design, 187–190, 2003.
- [5] A. Satoko, Y. Kazuya, "Adaptive Reaction Control for Space Robotic Applications with Dynamic Model Uncertainty," Advanced Robotics, 1099-1126, 2010.
- [6] J.L. Zhong, "Dynamic Modeling and Vibration Control of a Space Flexible Manipulator using Piezoelectric Actuators and Sensors," Advanced Materials Research, 46-52, 2011.
- [7] N. Nasiri, H. Sadjadianb, A.M. Shahri, "Nonlinear Stabilizing Controller for a Special Class of Single Link Flexible Joint Robots," Journal of Computer & Robotics 5, 1, 37-42, 2012.
- [8] A. Izadbakhsh, "Robust control design for rigid-link flexible-joint electrically driven robot subjected to constraint: theory and experimental verification," Nonlinear Dynamics, springer, 85, 2, 751–765, 2016.
- [9] N. Nasiri, H. Sadjadianb, A.M. Shahri, "Voltage-Based Control of a Flexible-Joint Electrically Driven Robot Using Backstepping Approach," 4th Power Electronics, Drive Systems & Technologies Conference (PEDSTC2013), Tehran, Iran, Feb 13-14, 2013.
- [10] W.J. Book, "Recursive lagrangian dynamics of flexible manipulator arms," Int. J. of Robotics Research, 87– 93, 1999.
- [11] F. Rakhsha, A.A. Goldenberg, "Dynamic Modeling of a Single Link Flexible Robot," Proc of the IEEE Int. Conf. on Robotics and Automation, 984–989, 1985.
- [12] A. Meghdari, F. Fahimi, "On the First-order Decoupling of Dynamical Equations of Motion for Elastic Multibody Systems as Applied to a Two-link Flexible Manipulator," Multibody Systems Dynamics, 1-20, 2001.
- [13] M.H. Korayem, H.N. Rahimi, "Nonlinear dynamic analysis for elastic robotic arms," Frontiers of Mechanical Engineering, 219- 228, 2008.
- [14] M.H. Korayem, H.N. Rahimi, A. Nikoobin, "Mathematical modeling and trajectory planning of mobile manipulators with flexible links and joints," Applied Mathematical Modeling, 3229-3244, 2012.
- [15] H.M. Aziz, j. Iqbal, "Flexible joint robotic manipulator: Modeling and design of robust control law," In Robotics and Artificial Intelligence (ICRAI), 2016 2nd International Conference on 2016 Nov 1, pp. 63-68. IEEE, 2016.
- [16] J. Jafari, M. Mirzaie, M. Zandbaf, "Mathematical Modeling and Nonlinear Dynamic Analysis of Flexible Manipulators using Finite Element Method," Universal Journal of Non-linear Mechanics, 56-61, 2013.
- [17] Y.C. Chang, H.M. Yen, "Robust tracking control for a class of electrically driven flexible-joint robots without velocity measurements," International journal of control, Taylor & Francis, 1; 85, 2, 194-212, 2012.
- [18] AL-Samarraie Sh. A., "Design of a Continuous Sliding Mode Controller for the Electronic Throttle Valve System". Journal of Engineering, Iraq, Baghdad University, No. 4, Vol. 17, pp.859-871 August, 2011.
- [19] Sh.A. AL-Samarraie and R.M. AL-Wardie, "Sliding Mode Controller for Electromechanical System with Chattering Attenuation," Al-Nahrain

University, College of Engineering Journal (NUCEJ), 18, 2, 208 – 218, 2015.

[20] M. Rubagotti, A. Estrada, F. Castaños, A. Ferrara and L. Fridman, "Integral Sliding Mode Control for Nonlinear Systems with Matched and Unmatched Perturbations," IEEE Transactions on Automatic Control, 56, 11, 2011.

[21] Sh.A. AL-Samarraie, M.H. Mishary, "High Order Sliding Mode Observer-Based Output Feedback Controller Design for Electro-Hydraulic System," Al-Khwarizmi Engineering Journal. 18, 12, 4, 1-1, 2017.

[22] Sh.A. AL-Samarraie and B.F. Midhat, "Sliding Mode Controller Design for a Crane Container System," Iraqi Journal of Computers, Communication and Control & Systems Engineering, 14, 1, 58-71, 2014.

[23] https://courses.engr.illinois.edu/ece486/Labs/Lab4/Kuo_article. Section 4-5 Sensors and Encoders in Control Systems 161.pdf. Downloaded at 6/3/2017.

[24] F. Castaños and L. Fridman, "Analysis and Design of Integral Sliding Manifolds for Systems with Unmatched Perturbations," IEEE Trans. Autom. Control, 51, 5, 853–858, 2006.

[25] V.I. Utkin, J. Guldner and J. Shi, "Sliding Mode Control in Electro-Mechanical Systems," CRC Press. Taylor & Francis Group, 2009.

[26] <https://www.intechopen.com/source/html/17687/media/image63.png>. Downloaded at 24/5/2017.

[27] V. Singh, V. Sharma, "Sliding Mode Controller Design for Controlling the Speed of a DC Motor," International Journal of Advanced Computing and Electronics Technology, Vol. 2, Issue 1, 2015.

[28] H. Brandtstadter and m. Buss, "Control of Electromechanical Systems using Sliding Mode Techniques," Proceedings of the 44th IEEE Conference on Decision and Control, and the European Control Conference, Seville, Spain, December 12-15, 2005.

[29] H.K. Khalil, "Nonlinear systems," 3rd Edition, Prentice Hall, USA, 2002.

[30] F.H. Clarke, "Optimization and non-smooth analysis," Society for Industrial and Applied Mathematics; 1990.